IJE TRANSACTIONS B: Applications Vol. 39, No. 05, (May 2026) 1077-1087

International Journal of Engineering

Journal Homepage: www.ije.ir

Mathematical Modeling of a Hydro-mechanical System with a Positive Displacement Motor and Hydraulic Thruster to Optimize the Drilling Process for Extended-reach Drilling Wells

G. V. Buslaev[a], A. V. Konoplyannikov*[b]

[a] *Laboratory of Thermodynamic, Gas Chemical and Energy Processes of Oil and Gas Production of the "Arctic" Research Center, Empress Catherine II Saint Petersburg Mining University, Russia*

[b] *Department of Well Drilling, Empress Catherine II Saint Petersburg Mining University, Russia*

PAPER INFO

Paper history:
Received 18 April 2025
Received in revised form 27 May 2025
Accepted 28 June 2025

Keywords:
Drilling
Hydraulic Thruster
Positive Displacement Motor
Mathematical Model
Axial Force
Extended-Reach Drilling Well
Drilling Optimization

ABSTRACT

This study addresses key challenges in Extended-Reach Drilling operations, focusing on limited axial load transfer to the bit and increased hydraulic pressure losses. These issues are critical as they directly impact drilling efficiency and well construction capabilities. A technological solution involving the integration of a hydraulic thruster into the bottomhole assembly was proposed and investigated. A comprehensive mathematical model of the hydromechanical system comprising the bit, Positive Displacement Motor (PDM), hydraulic thruster and mud pump was developed. An iterative computational algorithm in Python was created for equipment selection and drilling regime optimization. The novelty of the work lies in the development of a comprehensive modeling approach that integrates the operation of a hydraulic thruster with a PDM within the bottom hole assembly and mud pump. This research provides a scientifically grounded methodology for designing bottomhole assembly (BHA) with integrated hydraulic thrusters, filling a gap in existing literature. The study confirms the effectiveness of hydraulic thruster applications in drilling deep, deviated, and horizontal wells.

***doi**: 10.5829/ije.2026.39.05b.03*

Graphical Abstract

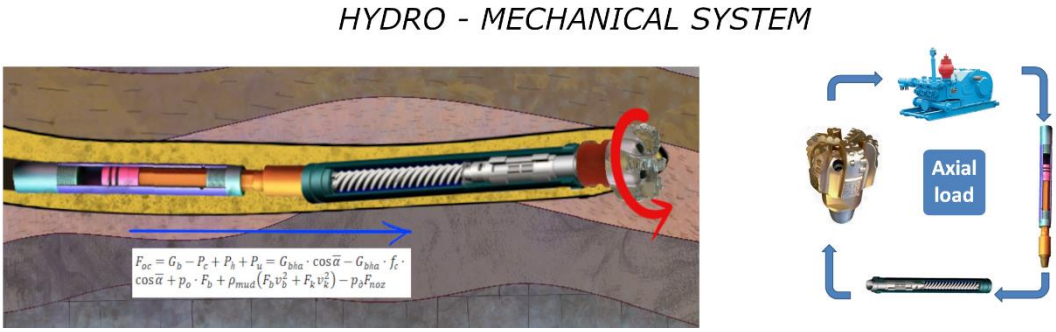

1. INTRODUCTION

In the early stages of oil and gas production, drilling was limited exclusively to vertical wells. The primary objective of drilling operations was to reach target depths and expose hydrocarbon-bearing formations. Precise spatial positioning of the wellbore trajectory was not considered a significant concern (1).

Advances in drilling technology enabled the construction of deviated directional wells. The ability to

*Corresponding Author Email: konoplyannikovaleksandr@gmail.com (A.V. Konoplyannikov)

Please cite this article as: Buslaev GV, Konoplyannikov AV. Mathematical Modeling of a Hydro-mechanical System with a Positive Displacement Motor and Hydraulic Thruster to Optimize the Drilling Process for Extended-reach Drilling Wells. International Journal of Engineering, Transactions B: Applications. 2026;39(05):1077-87.

drill complex well profiles—with multiple angle build-up, drop-off, and stabilization sections—emerged thanks to downhole surveying tools capable of taking measurements while drilling (MWD) (2). This process requires precise tools, real-time data acquisition, and control systems to monitor and adjust the well trajectory promptly. The development of directional drilling technology has set records for extended horizontal sections, making it possible to construct wells exceeding 15,000 meters in drilled depth, both onshore and offshore (3).

Although Extended-Reach Drilling (ERD) offers numerous operational advantages over conventional directional wells (4), it presents several technical challenges during well construction, including poor cuttings removal, insufficient weight transfer to the bit, increased hydraulic resistance and torque, and elevated equivalent circulating density (ECD) (5).

The PDM have been widely used for drilling directional and deep wells since the mid-century. The PDM design incorporates a “rotor-stator” pair. The rotor has a helical screw-shaped geometry. The stator’s inner surface is coated with a vulcanized elastomer that matches the rotor’s geometry and transmits reactive torque to the rotor through the flow of drilling mud.

PDMs are suitable for high-rate drilling with various bit types, including roller-cone, diamond, and PDC bits. However, PDMs are sensitive to hot, abrasive, and corrosive environments (6) due to the elastomer lining of the stator.

Drilling extended deviated and horizontal wells poses challenges related to the inability to maintain consistent bit weight and instability caused by oscillations and poor wellbore trajectory control. Modern engineering solutions include: (a) devices generating induced pulses or resonators that create vibrations in the BHA system (7, 8); and (b) BHA components combined with technological measures to enhance well trajectory accuracy (9).

To improve drilling quality in wells with extended horizontal sections, it is proposed to incorporate Rotary Steerable Systems (RSS) into the BHA (10, 11). The RSS may be used with or without a PDM section (12). Although RSS is used to drill most ERD wells, several wells with measured depths exceeding 11,000 meters have been successfully drilled using PDMs (13).

It should be noted that directional and horizontal well drilling with PDMs involves alternating between rotary mode (with drillstring rotation) and sliding mode (without rotation) to maintain the planned well trajectory and correct local deviations caused by rock anisotropy (14, 15). However, as the horizontal section length increases, substantial frictional resistance develops due to contact between the non-rotating drillstring and the wellbore wall (16-18).

At well depths and curvatures where frictional losses and drag forces approach the axial load exerted by the BHA on the bit (19), transferring weight from the surface becomes inefficient or even impossible (20).

In such cases, downhole bit wieght control systems integrated into the BHA offer a significant advantage, eliminating the need for weight transfer through the drillstring (21). This approach allows for shortening the BHA by reducing the number of heavy-weight drill pipes (HWDP), which in turn positively impacts the equivalent circulating density (ECD).

ECD can be controlled by regulating the drilling mud flow rate in the drillpipe annulus and minimizing tool joint friction losses. However, this approach complicates cuttings transport and can cause ECD fluctuations, potentially resulting in lost circulation and wellbore breathing (22), while also negatively impacting the near-wellbore formation (23-25). Cuttings accumulation on the low side of the wellbore reduces the effective flow area, increasing pressure differentials. Pressure losses in the annular space have been observed to rise with increasing drillstring rotation speeds (26, 27). Notably, pressure differentials within the drillstring assembly have little effect on annular ECD (28, 29).

The technologies employed in ERD well drilling—such as lubricant additives in drilling fluids, RSS, and oscillators—cannot fully eliminate drag forces. Consequently, as the wellbore deviation from vertical increases, there will always be a limitation in delivering sufficient weight on bit (WOB) for effective rock destruction.

This paper proposes addressing the aforementioned challenges through integration of a hydraulic thruster into the BHA. By optimizing mud pump flow rates, selecting appropriate PDM specifications, and adjusting bit nozzle diameters, significant improvements in bit performance can be achieved. Additionally, separating BHA components using a hydraulic thruster helps to reduce bit-induced vibrations (30).

Analysis of bit dynamics under various drilling methods has demonstrated that vibrations in the BHA and drillstring originate from tool rotation and its interaction with both formation rock and wellbore walls. These vibrations manifest as axial, lateral, and torsional oscillations, which arise under certain drilling conditions—such as excessive bit weight or specific rotational speeds (31). These effects can lead to tool instability, bit balling of PDC cutters, and other performance-degrading phenomena (32-34).

To optimize PDC bit performance and mitigate vibrations, the scientific literature extensively explores cutting structure control systems and methods for determining weight on bit (WOB). These developments aim to regulate the stress-dynamic environment in both the drillstring and BHA, thereby improving overall drilling efficiency (35).

Researchers from Freiberg University of Mining and Technology developed a hydraulic thruster with a diaphragm and choke (Shockspear) featuring a replaceable sleeve for pressure regulation. The methodology for calculating its parameters was successfully applied to drilling Emmen-9 well in a fractured carbonate reservoir, achieving a 4400 m borehole with 2000 m deviation.

In 2006, researchers at Ukhta State Technical University, Buslaev and Belkin (36) developed a multifunctional downhole feed system (DFS) that combines the functions of a shock absorber, oscillation compensator, and hydraulic thruster. Prototype testing confirmed reduced vibration levels and improved bit weight transfer.

Field trials of the "ZUPD-195" in hard rock formations at depths greater than 3000 m increased bit run length from 7.5 m to 29.2 m, while reducing bit wear and non-productive time (NPT) by a factor of four. The drillstring weight was reduced from 300 kN to 100 kN, resulting in a time saving of 49.42 hours. Although further testing is needed for comprehensive evaluation, the results confirm the system's effectiveness (36).

Research was patented a hydraulic thruster connected to a PDM via a hollow rod shaped as a multi-start helical rotor. The rotor engages with a helically profiled stator mounted on the rotor, both sharing identical planar and spatial geometry.

The effectiveness of hydraulic thrusters was confirmed by 2020 field trials in China, which showed a 50% increase in rate of penetration (ROP) compared to offset wells and data reported by Zhao and Cui (37).

The use of hydraulic thrusters—downhole feed systems (DFS) integrated into the BHA—addresses several challenges encountered during ERD well construction. As these downhole tools convert hydraulic energy into axial force, optimizing drilling mud flow rate and bit nozzle diameter enables a significant increase in weight-on-bit (WOB) without the need to lengthen the BHA for mass-based loading.

In "pressure relief" mode, the hydraulic thruster isolates the lower BHA from the rest of the drillstring, maintaining a constant, controlled WOB while reducing axial vibrations and shock loads. The lack of a rigid connection with the upper BHA minimizes transmission of vibrational loads. Additionally, the DFS helps prevent stuck pipe incidents by generating vertical impacts and inducing rapid pressure surges in the system.

DFS systems are compatible with both rotary steerable systems (RSS) and positive displacement motors (PDM).

Table 1 summarized the analysis hydraulic thruster components which are well-studied and field tests confirm their operational reliability, there is a lack of methodological frameworks for modeling their interaction with other BHA elements. The absence of scientifically grounded design principles for BHAs with integrated hydraulic thrusters remains a key limitation to the widespread adoption of these systems.

This paper presents a study focused on integrating the operation of a hydraulic thruster and a positive displacement motor (PDM) within the BHA.

2. METHODOLOGY

When using a hydraulic thruster in the well drilling process, the principle of drilling control differs from conventional drilling technology. The key distinction lies in the ability to regulate the bit weight by adjusting the flow rate of the drilling mud. This imposes specific constraints on the operational regime of the downhole motor (PDM).

The study introduces a boundary condition in which the conventional drill string is modeled as a suspended assembly, divided by a hydroulic thruster device into two distinct sections:

The upper section of the drill string, suspended from the hoisting system during drilling, features a free lower end equipped with the device housing. To increase applied load via gravitational force contribution, the housing may alternatively rest on the Lower BHA (LBHA). LBHA mobile drill section, with its bottom end (bit) in contact with the borehole bottom during drilling.

TABLE 1. Testing Results of Hydraulic Thruster Devices

Technology	Formations	Drilling Interval (m)	Effect
"ZUPD -195"+rotory (36)	Severniy Ugid (Russia)	3321 - 3250	increasing the drill bit footage and reducing the number HWDP in the BHA.
"Hydra-Thrust" + PMD (38)	Mahogany (Gulf of Mexico)	120 - 4265	average improvement of penetration rates of 35-5% while both sliding and rotating respectively.
"Thruster Device" + PMD (39)	Emmen-9 (Netherland)	4212 -4505	average increased ROP from 6.7 m/h to 10 m/h
"165mm hydraulic thruster" + PMD (37)	Tao-2 (China)	2146 - 2600	the average mechanical drilling rate wasincreased by about 50%; the footage of a single bit has been increased from 251 meters to 454 meters.

The opposing end incorporates a telescoping shaft capable of axial displacement within the device stroke length along the wellbore axis.

The development of a computational mathematical model for the hydro-mechanical system "bit – downhole motor – hydraulic thruster – mud pump" to determine the final values of axial WOB, rotary speed, and torque on the bit is a relevant research objective.

In Figure 1 A, C – in vertical wells; B, D – in horizontal wells; A, C – with manual load application; B, D – with automated load application; 1 – Bit; 2 – Stabilizer; 3 – Downhole motor (PDM); 4 – Centralizer; 5 – Heavy-weight drill pipe (HWDP); 6 – Drill pipes; 7 – Kelly; 8– Extendable shaft of the hydraulic thruster; 9 – Hydraulic thruster body.

In general form, accounting for all factors except torque and drill string dynamics. This simplification is justified by the altered operational mode of the drill string and the capability to compensate for axial oscillations through displacement of the lower mobile drill section (LBHA) relative to the drill pipe column. This approach effectively eliminates the influence of dynamic processes in the drill string on the axial component of bit load. The axial weight on bit (WOB) is given by (kN):

$$P_{oc} = G_b - P_c + P_h + P_u \quad (1)$$

G_b – axial component of the buoyed weight of the bottomhole assembly (BHA), including heavy-weight drill pipes (HWDP), extendable shaft of the hydraulic thruster, downhole motor (PDM), bit, stabilizers, and other elements in the drilling mud (kN):

$$G_b = G_{bha} \cdot cos\,\overline{\alpha}, \quad (2)$$

G_{bha} – weight of the BHA section used to apply WOB in conventional drilling or the buoyed weight of the movable BHA when using a downhole bit feed device (kN).

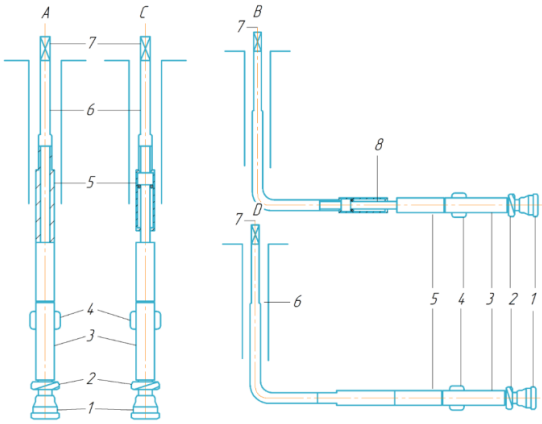

Figure 1. Schematic of axial WOB generation in horizontal wells

$\overline{\alpha}$ – average zenith angle over the BHA section (°).

P_c – resistance force opposing WOB transfer to the bit (kN):

$$P_c = f_c \cdot N = f_c \cdot G_{bha} \cdot sin\,\overline{\alpha}, \quad (3)$$

N – wellbore wall reaction force to the perpendicular component of the BHA weight (kN).

f_c – generalized coefficient of resistance forces, accounting for friction, tool joint wall contact, differential sticking, and other factors.

P_h – hydraulic component of WOB. Excluded in conventional drilling (as it induces internal tension) but included for downhole feed devices, where it becomes the primary WOB component (kN).

F_{noz} – total flow area of bit nozzles (m²).

$$P_h = p_o \cdot F_b - p_{bit}F_{noz} - p_{pdm}F_b \quad (4)$$

p_o – pressure differential between the extendable shaft cavity and annular pressure at the piston level (MPa):

$$p_o = p_{bit} + p_{pdm} + p_y + p_{ht} + p_{an} \quad (5)$$

$p_{bit}, p_{pdm}, p_y, p_{ht}, p_{an}$– hydraulic losses in the bit, downhole motor (PDM), downhole feed device, pipes, and annular space below the device (MPa).

F_b– inner cross-sectional area of the PDM body (or HWDP in rotary drilling); for feed devices, this equals the piston area (m²).

P_u– inertial force component due to drilling mud momentum (kN):

$$P_u = \rho_{mud}(F_b v_b^2 + F_k v_k^2), \quad (6)$$

ρ_{mud} – drilling mud density (kg/m³); v_b, v_k – fluid velocity inside the drill string and annular space, respectively (m/s); F_b, F_k – cross-sectional area of the pipe inner diameter and annular space, respectively (m²).

2. 1. Determination of Bit Torque Under Given WOB and Rotary Speed The torque at the bit depends on multiple factors, the primary ones being the bit type, cutting structure aggressiveness, and rotary speed. According to Plotnikov V.M.:

$$M_{bit} = m \cdot G \quad (7)$$

M_{bit}– Torque at the bit (N·m); m – Specific torque per unit WOB (min⁻¹); G – axial weight on bit (WOB) (N). The specific torque can be estimated using a simplified empirical formula proposed by Simonyants:

$$m = a_{dem}\left[\frac{28}{n} + 0{,}14\right]D_{bit}^2 \quad (8)$$

a_{dem}– Dimensionless coefficient dependent on bit type; n – Bit rotary speed (rpm); D_{bit} – Bit diameter (m).

For research purposes, the dimensionless coefficient can be approximated within the following ranges for different bit types and formations:

2. 2. Determination of Pressure Drop in a Positive Displacement Motor (PDM) **A**n analysis of bench test results established that the pressure loss (p_{pdm}) in a PDM depends on the bit torque (m), average drilling mud flow velocity between the rotor and stator, PDM displacement volume (V_{pdm}), drilling mud density, and radial interference. The relationship is expressed as follows:

$$p_{pdm} = \frac{\rho Q_{pdm}^2}{f^2}\left[a_1 + b_1\left(\frac{mf^2}{Q^2 V_{pdm}\rho}\right)^{c_4}\right] \quad (9)$$

Q_{pdm} – drilling mud flow rate through the PDM (m³/s); ρ – drilling mud density (kg/m³); f – Cross-sectional flow area between the rotor and stator (m²); V_{pdm} – PDM displacement volume (m³); m – Output shaft torque (N·m).

a_p, b_p, c_p – Empirical coefficients for pressure drop calculation:

$$a_p = 5{,}689 + 0{,}831103 \cdot 10^3 \cdot \frac{\delta}{V_{\text{pdm}}^{1/3}} + 0{,}262323 \cdot 10^6 \cdot \left(\frac{\delta}{V_{\text{pdm}}^{1/3}}\right)^2 \quad (10)$$

$$b_p = 9{,}02793 - 0{,}280917 \cdot 10^3 \cdot \frac{\delta}{V_{\text{pdm}}^{1/3}} + 0{,}028979 \cdot 10^6 \cdot \left(\frac{\delta}{V_{\text{pdm}}^{1/3}}\right)^2 \quad (11)$$

$$c_p = 1{,}1958 + 0{,}042242 \cdot 10^3 \cdot \frac{\delta}{V_{\text{pdm}}^{1/3}} - 0{,}0043379 \cdot 10^6 \cdot \left(\frac{\delta}{V_{\text{pdm}}^{1/3}}\right)^2 \quad (12)$$

Here, δ represents the radial interference (positive values) or clearance (negative values), which depends on the output shaft torque and the wear condition of the helical rotor-stator pair (m).

2. 3. Determination of PDM Rotary Speed The rotational speed of the PDM output shaft depends on the bit torque (m), similar to how the pressure drop $p_{\text{ВЗД}} = f(m)$ characterizes PDM performance. The shaft speed is influenced by drilling mud flow rate, density, displacement volume, and radial interference:

$$n = \frac{Q_{pdm}}{V_{pdm}^{1/3} f}\left[a_n + b_n\left(\frac{mf^2}{Q^2 V_{pdm}\rho}\right)^{c_4}\right] \quad (13)$$

TABLE 2. Dependence of Coefficient a_{dem} on Bit Type and Rock Formation

Rock Formation	Roller-cone bit	Diamond bit	PDC bit
Soft to medium	0,9…1,0	-	3,4…3,5
Medium to hard	0,7…0,8	-	3,0…3,3
Hard to abrasive	0,5…0,6	1,8…2,5	-

TABLE 3. Example of Calculated Pressure Drops for Different Radial Interference Values

M, *N·m*	Radial interference/clearance δ, *m*				
	-0,6·10⁻³	**-0,3·10⁻³**	**0**	**0,3·10⁻³**	**0,6·10⁻³**
0	0,82	0,85	0,90	1,10	1,50
500	1,16	1,18	1,20	1,37	1,77
1000	1,54	1,50	1,50	1,72	2,15
1500	1,88	1,90	1,83	2,05	2,46
2000	2,25	2,26	2,23	2,40	2,86
2500	2,69	2,68	2,68	2,84	3,40
3000	3,10	3,06	3,12	3,33	3,63
3500	3,50	3,55	3,62	3,88	4,12
4000	4,00	3,90	4,15	4,40	4,65
4500	-	4,40	4,68	5,00	5,15
5000	-	4,95	5,30	5,60	5,80
5500	-	-	-	-	6,50

a_n, b_n, c_n – empirical coefficients for shaft speed calculation:

$$a_n = 3{,}402 \cdot 10^{-2} + 0{,}000749 \cdot 10^3 \cdot \frac{\delta}{V_{pdm}^{1/3}} - 0{,}000149 \cdot 10^6 \cdot \left(\frac{\delta}{V_{pdm}^{1/3}}\right)^2 \quad (14)$$

$$b_n = -0{,}89119 \cdot 10^{-2} + 1{,}53166 \cdot \frac{\delta}{V_{pdm}^{1/3}} + 0{,}01911751 \cdot 10^4 \cdot \left(\frac{\delta}{V_{pdm}^{1/3}}\right)^2 \quad (15)$$

$$c_n = 1{,}32618 + 0{,}0756845 \cdot 10^3 \cdot \frac{\delta}{V_{pdm}^{1/3}} + 0{,}013533 \cdot 10^6 \cdot \left(\frac{\delta}{V_{pdm}^{1/3}}\right)^2 \quad (16)$$

2. 4. Algorithm of the Mathematical Model for the Drilling System When drilling with a hydraulic thruster, the axial weight on bit (WOB) is functionally dependent on multiple parameters. The general interaction scheme of the hydro-mechanical system components is shown in Figure 2.

The interactions between system elements create complex functional dependencies.

nitial Conditions of the Hydro-mechanical System:

PDM₀: $p_{pdm} = p_{0pdm}$

$n_{pdm} = n_{0pdm}$

Hydraulic Thruster₀: $F_{oc} = (p_{bit} + p_{pdm} + p_{an}) * S$

Drill Bit₀: $p_{bit} = f(Q)$

$m_0 = f(F_{oc}, n)$

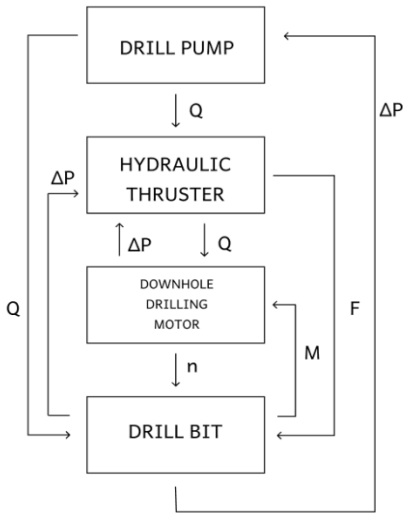

Figure 2. Schematic of the mathematical model

IThe pump flow rate (Q) is selected to ensure the required axial load, enhance wellbore cleaning efficiency, and maintain continuous operation of the PDM. Pressure losses in the drillstring and annular space (p_{an}) were calculated using a viscoplastic fluid model. The Shvedov–Bingham model was used to describe the behavior of the viscoplastic drilling fluid.

The system efficiency coefficient is defined as the ratio of useful hydraulic energy to mechanical energy, expressed as a percentage (40). The Shvedov – Bingham model is widely used to describe the rheological behavior of drilling fluids. The model assumes that the fluid begins to flow only after overcoming a critical shear stress (yield point, τ_0). The model is described by two parameters: plastic viscosity (μ_p) – resistance to flow after the onset of motion; yield point (τ_0) – the minimum stress required to initiate flow. The model accurately predicts hydraulic losses in annular spaces and pipes compared to Newtonian models. Despite its advantages, the model does not account for: thixotropy (time-dependent viscosity changes); complex effects at high shear rates (e.g., turbulence).

System performance analysis identified three key interdependent parameters that govern overall productivity. A critical feature of the system is the initial pressure drop of the drilling fluid in the hydraulic thruster, which generates additional axial load at the bit.

The most sensitive component to axial load fluctuations is the PDC bit, which remains in direct contact with the bottomhole Due to the bit's shearing–crushing action, increased axial load results in deeper cutter penetration into the rock. This significantly complicates the mechanical rock-breaking process and leads to a considerable increase in reactive torque at the bit.

The rising reactive torque is transferred to the motor shaft, hindering its rotation and increasing pressure drop within the motor's working chamber. This elevated system pressure drop subsequently impacts the hydraulic thruster, further increasing axial load at the bit. As a result, the system enters a self-sustaining feedback loop.

It is important to note that this sequence of system interactions forms a continuous feedback chain, in which any change in one parameter inevitably requires adjustments to other operational characteristics of the system.

3. RESULTS CALCULATION

The following initial data were used for the calculations (see Table 4). The computational model was implemented in Python using an iterative algorithm based on the mathematical formulations described in the Methodology section. The iterative algorithm analyzes key parameters: bit torque, PDM spindle speed, and axial load generated by the hydraulic thruster.

As an example, the iterative calculation results for Q = 0.028 m³/s are presented Table 5. The iteration process was deemed convergent upon satisfying the following criterion: the relative change in the load applied by the hydraulic actuator and the rotational speed of the downhole motor. The convergence threshold was set at 1e-3, with a maximum iteration count of 100.

The relationship between rotational speed and applied torque is attributed to seal failure in helical channels due to working fluid leakage. This phenomenon causes speed variations depending on torque magnitude. The system parameters stabilize, reaching a steady-state operating regime.

The study of bit load dependence on flow rate is crucial for analyzing the hydraulic thruster's performance. Using the axial load graph, we examine the system's initial and equilibrium states obtained from simulations within the flow rate range Q = 0.042 – 0.001 m³/s.

The dependence of rotational speed on applied torque is caused by loss of sealing in the helical channels due to working fluid leakage. This phenomenon leads to speed variation as a function of torque magnitude. The system parameters reach equilibrium, resulting in stable operating conditions.

The investigation of bit load dependence on drilling mud flow rate represents a critical stage in analyzing the hydraulic thruster's performance. Using the axial load graph Figure 3, we examine the system's initial and equilibrium states obtained through modeling within the flow rate range Q = 0.042-0.001 m³/s:

The red curve indicates initial load at bit-bottomhole contact, while the blue curve shows final load after hydro-mechanical system stabilization.

TABLE 4. Initial Calculation Data

Input Parameter	Value	Input Parameter	Value
Bit Parameters		***Drill Pipe Parametrs***	
Dimensionless bit-type coefficient	3.0	Drill pipe length, m	12
Bit diameter, m	0.1905	Outer diameter of drill pipe, m	0.127
Number of nozzle jets	6	Inner diameter of drill pipe, m	0.1140
Nozzle diameter, m	0.012	Tool joint outer diameter, m	0.166
Bit weight, kg	40	Total drill string length, m	2500
Rotary speed, rpm	30	***Hydraulic Thruster Parameters***	
Drilling mud Parameters		HT inner diameter, m	0.152
Density, kg/m³	1200	Piston diameter of HT, m	0.110
Plastic viscosity	0.01	HT shaft weight, kg	500
Dynamic viscosity	5	***Well Parameters***	
PDM Parameters		Well inclination angle, °	0
Rotor lobe count	9	Friction coefficient	0.3
Stator lobe count	10	Casing inner diameter, m	0.2699
PDM outer diameter, m	0.172	Cased interval length, m	2000
Thread pitch coefficient	4	Open hole diameter, m	0.210
PDM weight, kg	500	Open hole interval length, m	500

The results of mathematical modeling demonstrate that this relationship increases in direct proportion to the drilling fluid flow rate.

The red curve (Figure 3) indicates initial load at bit-bottomhole contact, while the blue curve shows final load after hydro-mechanical system stabilization.

Mathematical modeling results demonstrate that this relationship follows a directly proportional function and decreases monotonically.

Figure 4 presents calculated dependencies of well inclination angle versus both bit load (generated by the hydraulic thruster) and bit rotational speed at a fixed pump flow rate Q = 0.028 m³/s.

Figure 5 displays the hydro-mechanical system's torque (N•m) and rotational speed (rpm) as functions of working fluid flow rate (m³/s). Analysis reveals the correlation between these key parameters. The intersection point corresponds to maximum efficiency.

Figure 6 shows overall system efficiency (%) as a function of fluid flow rate (m³/s). The vertical axisrepresents efficiency values (14% to 19%), while the horizontal axis indicates flow rates ranging from 0.0225 m³/s to 0.0425 m³/s. The data demonstrate an inverse relationship between flow rate and system efficiency. Peak efficiency (19%) occurs at 0.023 m³/s, decreasing to 14% at maximum flow (0.0425 m³/s). This trend suggests either energy losses or suboptimal equipment configuration.

TABLE 5. Iterative Calculation Results

Iteration No	PDM Speed, rpm	Axial Load from Hydraulic Thruster, N	Bit Torque, N•m	PDM Pressure Drop, KPa
1	126	32769	1137	1323.5
2	120	38594	1345	1875.9
3	116	40842	1417	2092.2
4	115	41194	1485	2129.3
5	115	41216	1489	2131.7

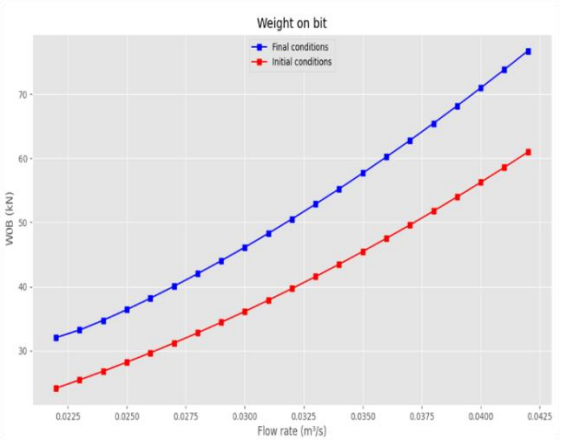

Figure 3. Thruster load as a function of mud pump flow rate

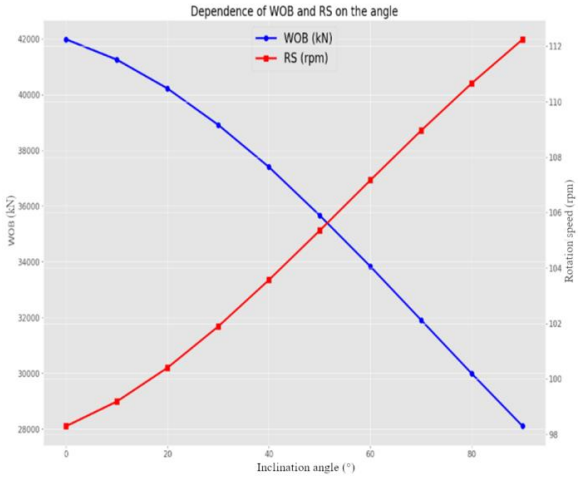

Figure 4. Relationship between rotational speed/load and well inclination angle

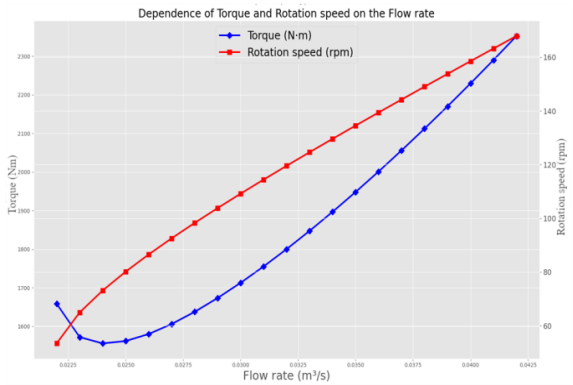

Figure 5. Torque and rotational speed versus drilling mud flow rate

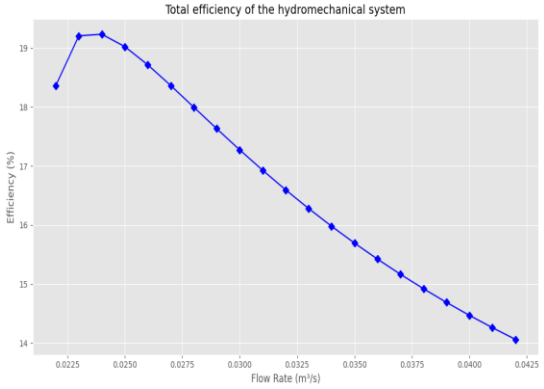

Figure 6. Hydro-mechanical system efficiency versus drilling mud flow rate

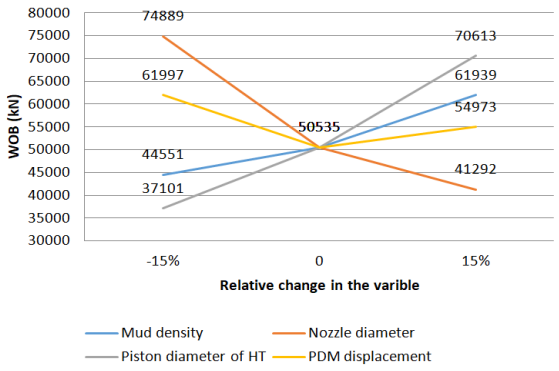

Figure 7. Sensitivity analysis

TABLE 6. Parameters for sensitivity analysis

Flow rate Q = 0.032 (m^3/s)			
Parameters	**-15%**	**0**	**15%**
Mud density (kg/m)	1020	1200	1380
Nozzle diameter (m)	0,01	0,012	0,014
Piston diameter of HT (m)	0,094	0,11	0,126
PDM displacement ($m^3 10^{-3}/s$)	11,56	13,6	15,6

4. DISCUSSION

Drilling with a hydraulic thruster and a Positive Displacement Motor (PDM) is a complex, yet technologically viable process. The complexity arises from the fact that both BHA components depend on well flushing parameters. Specifically, the bit torque depends on the axial load, which in turn affects the pressure drop across the PDM. This pressure drop defines the hydraulic component of the axial force generated by the downhole thruster. The incremental load resulting from the incremental torque is transmitted back to the bit, thereby closing the feedback loop.

This problem can be solved analytically, but the study employed an iterative computational algorithm, which allows for model refinement and increased complexity without requiring analytical solutions.

A comprehensive sensitivity analysis was conducted to evaluate the influence of four critical operational parameters on the hydraulic system's performance under a constant flow rate of 0.032 m³/s (Figure 7 and Table 6). The study employed a parametric variation approach (±15% deviation from baseline values) to systematically assess each parameter's individual and synergistic effects on WOB. The increase in density elevates hydraulic resistance, potentially influencing pressure losses and load distribution. During drilling operations, bit nozzles are subject to wear-induced diameter enlargement, which may reduce system WOB due to decreased pressure differential. The piston diameter and PDM displacement volume represent non-adjustable parameters during drilling operations, yet remain critical for load optimization during equipment selection and exert significant influence on system performance.

Accordingly, the model in this study was enhanced to account for the effect of bit rotational speed on bit torque. There is a correlation between the linear cutter velocity and the axial reaction force of the rock on the cutter face during cutting. Figure 8 demonstrates that as the cutter's relative velocity increases, the axial reaction force at the bottomhole also increases, leading to a reduction in single-cutter penetration depth.

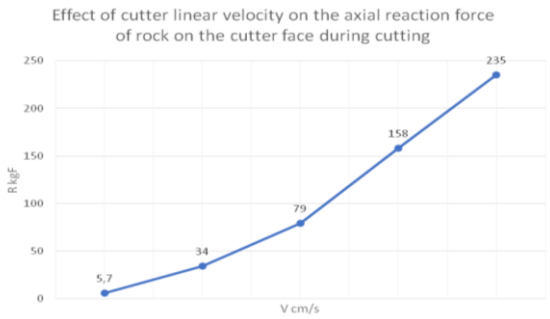

Figure 8. Effect of cutter linear velocity on the axial reaction force of rock on the cutter face during cutting

From a physical process perspective, the key aspect lies in the interaction between hydrodynamic and mechanical system components. During hydraulic thruster operation, drilling fluid flow energy is converted into axial mechanical load through a complex system of hydrodynamic resistances. Crucially, a feedback mechanism exists between WOB and flow characteristics: increased axial load generates (see Equation 8) higher reactive torque, which subsequently affects the pressure differential across PDM and thruster performance parameters. Importantly, increased PDM torque reduces rotational speed, thereby altering the relationship between bit torque and generated axial load.

In turn, the bit rotational speed at a given pump flow rate depends on the PDM torque (see Equation 13).

The use of a numerical solution method allowed for the incorporation of this new influencing factor into the system's behavior, and the computational results are presented in Figures 3 to 6.

Optimization of BHA parameters with a hydraulic thruster requires selection of nozzle sizes and piston diameters capable of generating the designed WOB. For standard 215.9 mm bits, typical WOB ranges between 100-120 kN for roller cone bits and 50-70 kN for PDC bits. While field tests (Table 1) have demonstrated successful hydroulic thruster performance across various regions, these trials lacked downhole WOB measurement capabilities. Load estimation relied solely on hook load reduction - an indirect parameter that cannot accurately reflect actual bit force generation.

5. CONCLUSIONS

Based on a comprehensive analysis of theoretical and experimental data, and as part of research conducted under the state assignment of the Ministry of Science and Higher Education of the Russian Federation (FSRW-2023-0002), the following scientifically substantiated conclusions were obtained:

The effectiveness of hydraulic thruster applications in drilling deep, deviated, and horizontal wells has been theoretically proven and experimentally confirmed. The proposed modeling approach for the hydro-mechanical system "Bit – PDM – Hydraulic Thruster – Mud Pump" enables equipment selection and optimization of the well drilling regime. This solution is particularly significant when drilling wells with high deviations from vertical, where bit weight-on-bit (WOB) becomes a limiting factor for the achievable interval length. Calculations performed within the study demonstrated that the hydro-mechanical system can provide a WOB exceeding 72 kN during vertical drilling and over 32 kN in the horizontal section, excluding the weight of heavyweight drill pipes.

A mathematical model has been developed and successfully implemented, along with an iterative calculation algorithm coded in Python, which accounts for and integrates the key systems of the drilling assembly. The model allows for simulation and optimization of system and equipment parameters by varying input data and visualizing calculation results in the form of graphs and nomograms. The simulation results demonstrate high accuracy and convergence of the calculated data, confirming the reliability of the proposed model.

The modeling showed that when a hydraulic thruster is included in the BHA, the mud flow rate becomes the primary control parameter for regulating bit WOB and rotation speed.

The integration of a hydraulic thruster with a PDM enhances the operational scope of sliding-mode technology for trajectory adjustment in ERD wells. By enabling drill string reciprocation while maintaining toolface orientation, the thruster mitigates sticking risks during directional operations. Furthermore, in tight hole conditions or differential sticking scenarios, the thruster generates controlled upward/downward impulse loads, providing an alternative to conventional jarring tools, which exhibit limited efficacy in ERD applications.

The proposed solutions demonstrate significant practical value, as they not only enhance the efficiency of deviated and horizontal well drilling but also, under certain conditions, enable the long-term feasibility of drilling highly deviated wells using PDMs or RSS.The developed methodologies can be applied in the design of hydraulic thrusters and used for selecting PDM and bit parameters to optimize the drilling process.

The use of hydraulic thrusters opens new possibilities for advancing drilling technology in wells with high deviations from vertical. Further research may focus on optimizing the device design, expanding its operational range, and integrating it with intelligent drilling control systems.

6. REFERENCES

1. Wang H, Huang H, Bi W, Ji G, Zhou B, Zhuo L. Deep and ultra-deep oil and gas well drilling technologies: Progress and prospect. Natural Gas Industry B. 2022;9(2):141-57. 10.1016/j.ngib.2021.08.019
2. Zhdaneev OV, Zaytsev AV, Prodan TT. Possibilities for creating Russian high-tech bottomhole assembly. Записки Горного института. 2021;252:872-84. 10.31897/PMI.2021.6.9
3. Alzaki H, Rahmani N, Carr M, editors. Breaking ERD Records with Optimized Engineering and Practices: Making the Impossible Possible. SPE Middle East Oil and Gas Show and Conference; 2021: SPE. 10.2118/204550-MS
4. Panga M, Al Hammadi F, Marsh J, Mohamed A, Pace D, Wills J, editors. Ultra ERD Well Completions: Extending the Limits to Drive Profitability. Abu Dhabi International Petroleum Exhibition and Conference; 2023: SPE. 10.2118/216085-MS
5. Litvinenko V, Bowbrick I, Naumov I, Zaitseva Z. Global guidelines and requirements for professional competencies of

natural resource extraction engineers: Implications for ESG principles and sustainable development goals. Journal of Cleaner Production. 2022;338:130530. 10.1016/j.jclepro.2022.130530

6. Liagov I, Liagov A, Liagova A. Optimization of the Configuration of the Power Sections of Special Small-Sized Positive Displacement Motors for Deep-Penetrating Perforation Using the Technical System “Perfobore”. Applied Sciences. 2021;11(11):4977. 10.3390/app11114977
7. Zhong Z, Li Y, Zhao Y, Ju P. A Method of Evaluating the Effectiveness of a Hydraulic Oscillator in Horizontal Wells. Sound & Vibration. 2023;57(1):15-27. 10.32604/sv.2023.041954
8. Shi X, Huang W, Gao D, Zhu N, Li W. Extension limit analysis of drillstring with drag reduction oscillators in horizontal drilling. Geoenergy Science and Engineering. 2023;228:211996. 10.1016/j.geoen.2023.211996
9. Tian J, Mao L, Yang Y, Song H, Song J. Study on directional drilling coupling dynamics based on drill string rotary controller. Journal of Computational and Nonlinear Dynamics. 2023;18(9):091008. 10.1115/1.4062911
10. Li Y, Yu Y, Sun Y, Li B. Dynamics and fatigue life investigation of push-the-bit rotary steerable bottom hole assembly with whirling finite element model. Engineering Failure Analysis. 2023;150:107300. 10.1016/j.engfailanal.2023.107300
11. Никишин ВВ, Блинов ПА, Терехин ВА. Effectiveness of the method for selecting rotary-steerable systems based on the machine learning algorithm Random Forest Classifier. Bulletin of the Tomsk Polytechnic University Geo Assets Engineering. 2024;335(4):185-99. 10.18799/24131830/2024/4/4129
12. Litvinenko VS, Dvoynikov MV. Methodology for determining the parameters of drilling mode for directional straight sections of well using screw downhole motors. Записки Горного института. 2020;241:105-12. 10.31897/PMI.2020.1.105
13. El Sabeh K, Gaurina-Međimurec N, Mijić P, Medved I, Pašić B. Extended-reach drilling (ERD)—the main problems and current achievements. Applied Sciences. 2023;13(7):4112. 10.3390/app13074112
14. Wanpeng C, Danyang M, Yongmei G. Deep learning approach to prediction of drill-bit torque in directional drilling sliding mode: Energy saving. Measurement. 2025;250:117144. 10.1016/j.measurement.2025.117144
15. Barjini AH, Khoshnazar M, Moradi H. Design of a sliding mode controller for suppressing coupled axial & torsional vibrations in horizontal drill strings using Extended Kalman Filter. Journal of Sound and Vibration. 2024;586:118477. 10.1016/j.jsv.2024.118477
16. Zhang H, Ashok P, van Oort E, Shor R. Investigation of pipe rocking and agitator effectiveness on friction reduction during slide drilling. Journal of Petroleum Science and Engineering. 2021;204:108720. 10.1016/j.petrol.2021.108720
17. Shi X, Huang W, Gao D. Optimal design of drag reduction parameters with the rotary reciprocating control system and hydraulic oscillators in sliding drilling. Geoenergy Science and Engineering. 2024;243:212856. 10.1016/j.geoen.2024.212856.
18. El Sabeh K, Pašić B, Mijić P, Medved I. Reducing torque and drag in extended-reach wells using thermoplastic polymers for protective sliding rings. Applied Sciences. 2024;14(14):6161. 10.3390/app14146161
19. Sadeghi AN, Arıkan KB, Özbek ME. Modelling and controlling of drill string stick slip vibrations in an oil well drilling rig. Journal of Petroleum Science and Engineering. 2022;216:110759. 10.1016/j.petrol.2022.110759
20. Long Y, Wang X, Wang P, Zhang F. A method of reducing friction and improving the penetration rate by safely vibrating the drill-string at surface. Processes. 2023;11(4):1242. 10.3390/pr11041242
21. Li B, Zhu X, Dong L. Axial transfer characteristics of a drillstring in conjunction with bit penetration behavior in horizontal wells. Geoenergy Science and Engineering. 2024;240:212989. 10.1016/j.geoen.2024.212989
22. Islamov S, Islamov R, Shelukhov G, Sharifov A, Sultanbekov R, Ismakov R, et al. Fluid-loss control technology: From laboratory to well field. Processes. 2024;12(1):114. 10.3390/pr12010114
23. Raupov I, Rogachev M, Sytnik J. Overview of Modern Methods and Technologies for the Well Production of High-and Extra-High-Viscous Oil. Energies. 2025;18(6):1498. 10.3390/en18061498
24. Leushevaa E, Alikhanov N, Moradib ST. Experimental Evaluation of Influence of Physico-chemical Properties of Surfactants on Drilling Process in Pay-zones. International Journal of Engineering, Transactions A: Basics. 2025;38(4):819-29. 10.5829/ije.2025.38.04a.13
25. Nikitin V, Agrelkina M. Justification for the Selection of a Relative Permeability Model in the Task of Predicting Drilling Fluid Filtrate Invasion into the Formation. International Journal of Engineering Transactions A: Basics. 2025;38(10):2312-20. 10.5829/ije.2025.38.10a.08
26. Badrouchi F, Rasouli V, Badrouchi N. Impact of hole cleaning and drilling performance on the equivalent circulating density. Journal of Petroleum Science and Engineering. 2022;211:110150. 10.1016/j.petrol.2022.110150
27. Liu T, Leusheva E, Morenov V, Li L, Jiang G, Fang C, et al. Influence of polymer reagents in the drilling fluids on the efficiency of deviated and horizontal wells drilling. Energies. 2020;13(18):4704. 10.3390/en13184704
28. Dvoynikov MV, Minaev YD, Minibaev VV, Kambulov EY, Lamosov ME. Technology for killing gas wells at managed pressure. Известия Томского политехнического университета Инжиниринг георесурсов. 2024;335(1):7-18. 10.18799/24131830/2024/1/4315
29. Nikitin VI. Problem solution analysis on finding the velocity distribution for laminar flow of a non-linear viscous flushing fluid in the annular space of a well. Записки Горного института. 2022;258:964-75. 10.31897/PMI.2022.93
30. Tikhonov VS, Baldenko FD, Bukashkina OS, Liapidevskii VY. Effect of hydrodynamics on axial and torsional oscillations of a drillstring with using a positive displacement motor. Journal of Petroleum Science and Engineering. 2019;183:106423. 10.1016/j.petrol.2019.106423
31. Song J, Liu S, He Y, Jiang S, Zhou S, Zhu H. The state-of-the-art review on the drill pipe vibration. Geoenergy Science and Engineering. 2024;243:213337. 10.1016/j.geoen.2024.213337
32. Li X, Li M, Guo X, Agila W, Zhang H, Yang J. Influential mechanism of operational parameters on internal resonance of drill strings by numerical simulations. Engineering Research Express. 2024;6(4):045502. 10.1088/2631-8695/ad7cc9
33. Lalehparvar M, Vaziri V, Aphale SS, Wiercigroch M. Time delay effect in suppressing drill-string stick-slip vibration. IFAC-PapersOnLine. 2024;58(5):164-9. 10.1016/j.ifacol.2024.07.080
34. Volpi LP, Lobo DM, Ritto TG. A stochastic analysis of the coupled lateral–torsional drill string vibration. Nonlinear Dynamics. 2021;103(1):49-62. 10.1007/s11071-020-06099-z
35. Dvoynikov M, Kutuzov P. Analysis of efficiency of communication channels for monitoring and operational control of oil and gas wells drilling process. International Journal of Engineering, Transactions A: Basics. 2025;38(1):120-31. 10.5829/ije.2025.38.01a.12
36. Buslaev GV, Belkin AS, editors. Development and field testing of the downhole multi-purpose thrusting device for drilling of deep vertical and directional wells. SPE Russian Petroleum Technology Conference; 2015: SPE. 10.2118/176539-MS

37. Zhao J, Cui X, editors. Design and field test of hydraulic thruster. IOP Conference Series: Earth and Environmental Science; 2020: IOP Publishing. 10.1088/1755-1315/558/2/022067

38. Giles C, Seesahai T, Brooks J. Hydraulic thrusting devices improve drilling efficiencies. World Oil. 2001;222(9):59-64.

39. Reich M, Hoving P, Makohl F, editors. Drilling performance improvements using downhole thrusters. SPE/IADC Drilling Conference and Exhibition; 1995: SPE. 10.2118/29420-MS

40. Moradi SST. A probabilistic study on hole cleaning optimization. Записки Горного института. 2022;258:956-63. 10.31897/PMI.2022.67

Persian Abstract

چکیده

این مطالعه به بررسی چالش‌های کلیدی در عملیات حفاری با دسترسی گسترده (ERD) می‌پردازد و تمرکز آن بر انتقال محدود نیروی محوری به مته، افزایش افت فشار هیدرولیکی، و ارتعاشات رشته حفاری است. راه‌حل فناورانه پیشنهادی شامل ادغام یک تراستر (تقویت‌کننده) هیدرولیکی در مجموعه ابزار کف چاه (BHA) می‌باشد .یک مدل ریاضی از سامانه هیدرومکانیکی شامل مته، موتور جابجایی مثبت(PDM) ، تراستر هیدرولیکی، و پمپ گل طراحی شده است که در آن، ارتباطات بین اجزا و حالت‌های مختلف حفاری در نظر گرفته شده‌اند. الگوریتمی تکراری برای محاسبات عددی در محیط پایتون توسعه یافته است تا بهینه‌سازی پارامترهای حفاری را ممکن سازد .نتایج نشان می‌دهد که تراستر هیدرولیکی می‌تواند تا ۷۲ کیلونیوتن نیروی محوری در چاه‌های عمودی و ۳۲ کیلونیوتن در بخش‌های انحرافی تأمین کند، که این امر موجب بهبود کارایی فرآیند حفاری می‌گردد. این مدل می‌تواند به عنوان ابزاری جهت پشتیبانی از طراحی BHA و بهینه‌سازی پارامترهای حفاری مورد استفاده قرار گیرد و به‌ویژه در ساخت چاه‌های ERD از ارزش بالایی برخوردار است.